

## EQUILIBRIUM ISOTOPE FRACTIONATION

### Contents

3.1 Introduction.....	1
3.2 Theoretical determination of stable isotope fractionation factors.....	3
3.2.1 Free energy of reaction .....	3
3.2.2 The internal energy of a molecule .....	4
3.2.3 Vibrational Partition Function .....	5
3.2.4 Translational and Rotational Partition Function.....	7
3.2.5 The complete Partition Function Ratio .....	7
3.2.6 Extension to more complex molecules .....	8
3.2.7 ‘Empirical’ theoretical methods.....	8
3.3 Relationship to temperature .....	9
3.4 Experimental determination of fractionation factors .....	10
3.4.1 Introduction.....	10
3.4.2 Mineral-water exchange reactions .....	11
3.4.3 Mineral-calcite exchange reactions.....	13
3.4.4 Mineral-CO <sub>2</sub> exchange reactions .....	13
3.4.5 The three-phase approach .....	14
3.5 Empirical determination of fractionation factors.....	14
3.6 Other factors controlling isotope partitioning.....	15
3.6.1 Pressure effect.....	15
3.6.2 Oxidation state .....	16
3.6.3 Composition.....	17
3.6.4 Salinity .....	18
3.6.4 Polymorphism.....	18
3.7 Multiple isotope system: The “Big $\Delta$ ” notation .....	19
3.8 Distribution of isotopologues: Clumped Isotopes.....	22
References.....	24

Chapter 3

## EQUILIBRIUM ISOTOPE FRACTIONATION

### 3.1 Introduction

We can classify isotope exchange reactions as either kinetic or equilibrium. Kinetic reactions are irreversible, and by definition, cannot be treated using the methods of classical thermodynamics. Evaporation of water into unsaturated air cannot be reversed; the isotopic fractionation that occurs during evaporation is a combination of equilibrium fractionation and that related to the different translational velocities of the isotopologues of water. The extent of processes such as evaporation and diffusion can be calculated for certain conditions, using kinetic-based theories. Other kinetic isotope effects, such as those associated with bacterial metabolism, are extremely complex, and mostly defy quantification (although qualitative models can be constructed). Products from bacterial reaction tend to be enriched in the light isotope, because the dissociation energies are lower and bonds are more easily broken. As the title of this chapter suggests, we will not consider kinetic-based reactions at this point, although discussions of kinetic effects are addressed at various places in this book. The remainder of this chapter is devoted to quantifying the fractionation associated with reversible, equilibrium processes. Chacko *et al.* (2001b) provide an excellent detailed overview of the subject and should be consulted for additional information.

Many processes involving isotope exchange can be modeled by classical equilibrium thermodynamics, because they are near-equilibrium phenomena. High temperature processes, such as crystallization, generally approach isotopic equilibrium, as do a number of low temperature processes, including precipitation of *some* carbonate, phosphate and silica phases in water. Equilibrium fractionation between two phases is based on the differences in bond strength of the different isotopes of an element. The heavier isotope will form a stronger bond, and will be concentrated in the phase with higher bond energy or 'stiffness'. Qualitative rules for equilibrium isotope fractionation are given by Schauble (2004):

- 1) Equilibrium fractionation between two phases generally decreases with increasing temperature, proportional to  $1/T^2$ .
- 2) The degree of fractionation is generally larger for elements whose mass ratio is large  $\frac{m_{heavy} - m_{light}}{m_{heavy} m_{light}}$ , where  $m_{heavy}$  and  $m_{light}$  are the heavy and light isotopes, respectively. Therefore, the isotopes of lighter elements generally show larger fractionation than those of heavier elements.
- 3) The heavy isotope is preferentially partitioned into the site with the stiffest bonds (strong and short chemical bonds). Bond stiffness increases qualitatively for
  - a. high oxidation state, or high oxidation state in which the element is bonded,
  - b. lighter elements
  - c. covalent bonds

d. low coordination number.

From rule #1, fractionation varies regularly with temperature, which forms the basis for stable isotope thermometry. In order to have a *useful* isotope thermometer, we need to be able to measure the isotopic composition of the phases with the necessary precision, determine that they are indeed in isotopic equilibrium (often a daunting task), have a quantification of the fractionation as a function of temperature and have a mineral pair for which the fractionation changes significantly in response to temperature. In this chapter, we are concerned only with determining the fractionation factors. Quantification of fractionation factors has been made using three methods: 1) theoretical calculations based on statistical mechanics, 2) experimental determinations based on measured fractionations of phases equilibrated under known laboratory conditions, and 3) empirical calculations, based on measured fractionations of natural samples where independent temperature estimates can be obtained.

Each method of determining fractionation factors has benefits and limitations. Theoretical fractionation factors for simple gases have been calculated with a high degree of precision (Richet et al., 1977). At present, theoretical statistical mechanical calculations applied to complex minerals do not have the same precision as experimental determinations, although computational refinements continue to improve. A number of approximations must be made regarding the energy state of a phase because the quantum states of the individual molecules in solids and liquids do not behave independently from one another, and therefore approximate solutions to Schrödinger's equations cannot be used to calculate accurate fractionations (see Denbigh, 1971 for a general introduction). Also the magnitude of frequency shifts for the isotopically substituted molecule are not well known. However, the form of a theoretically-derived curves often allow for extrapolation of experimental fractionations beyond the temperature range of the experimental conditions. They may also be used for reactions that are difficult or impossible to duplicate in the laboratory, or have simply not-yet been done.

Experimental methods allow us to control most variables, such as temperature, reaction time, and chemical and isotopic composition. Experiments are difficult however, and many experiments are impractical, impeded by kinetic limitations. Empirical estimates take advantage of the fact that Nature provides us with very long-term experiments. A metamorphic rock heated to 500°C for 100 million years is an experiment that cannot be duplicated in the laboratory! At the same time, however, it is difficult to constrain temperatures very precisely in natural systems, and problems with isotopic inheritance and retrograde resetting always need be considered when empirical estimates are used. A nice website created by Georges Beaudoin and Pierre Therrien tabulates the results of a large number of published fractionations and allows for  $1000 \ln \alpha$  or temperatures to be estimated for any two phases. The site can be found at: <http://www2.ggl.ulaval.ca/cgi-bin/alphadelta/alphadelta.cgi> The reader should realize that this compilation does not assess the accuracy of each calibration and that it is appropriate to go back to the original sources to assess the reliability of relevant calibrations.

### 3.2 Theoretical determination of stable isotope fractionation factors

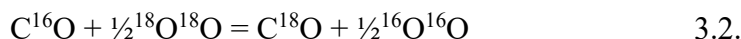
#### 3.2.1 Free energy of reaction

Fractionation factors can be calculated using the methods of statistical mechanics. The basic principles are not complicated, but the mathematics are complex, and only the basic concepts are presented here. The reader is referred to the following articles for additional details (Denbigh, 1971; Richet et al., 1977; O'Neil, 1986; Criss, 1999; Chacko et al., 2001a; Schauble, 2004).

The fundamental concept of the equilibrium exchange reaction was introduced in Chapter 2, section 4. A typical reaction is of the form



where  $A_1$  and  $A_2$  are the two isotopologues of the molecule  $A$ , with similar notation for molecule  $B$ . An example would be exchange between CO and O<sub>2</sub>, written as



$A_1$  is C<sup>16</sup>O,  $A_2$  is C<sup>18</sup>O,  $B_1$  is <sup>16</sup>O<sup>16</sup>O, and  $B_2$  is <sup>18</sup>O<sup>18</sup>O. Obviously the above reaction does not occur in nature as written. We do not have individual phases C<sup>16</sup>O and C<sup>18</sup>O, instead only one inseparable, mixed C<sup>18</sup>O – C<sup>16</sup>O phase. The reaction does make sense from a thermodynamic standpoint, however, because it is possible to assign activities to each of the components C<sup>16</sup>O, C<sup>18</sup>O, <sup>16</sup>O<sup>16</sup>O, and <sup>18</sup>O<sup>18</sup>O on the basis of concentrations. In this case, the equilibrium constant  $K$  is defined as

$$K = \frac{\prod (a_i)^{n_i}_{products}}{\prod (a_i)^{n_i}_{reactants}} = \frac{[a(^{16}O^{16}O)]^{1/2} a(C^{18}O)}{[a(^{18}O^{18}O)]^{1/2} a(C^{16}O)} \quad 3.3,$$

and because the activity coefficients are close to 1, equation 3.3 can be simplified as

$$K = \frac{\left(\frac{^{18}O}{^{16}O}\right)_{CO}}{\left(\frac{^{18}O}{^{16}O}\right)_{O_2}} = \alpha_{CO-O_2} \quad 3.4.$$

The equilibrium for exchange reaction 3.2 is given by

$$\Delta G_{r,T}^{\circ} = -RT \ln(K) \quad 3.5.$$

At 300 K,  $\alpha_{CO-O_2}$  is 1.028, so the free energy change for the reaction is -69 J (substituting  $\alpha$  for  $K$ ). Note that this energy change is miniscule compared to those

associated with chemical reactions. For the reaction  $\frac{1}{2}\text{O}_2 + \text{CO} = \text{CO}_2$ , for example, the free energy change (@ 298 K) is  $-257,200 \text{ J}$ .

### 3.2.2 The internal energy of a molecule

We can calculate the energy of a reaction by considering the total energy of each molecule in reaction 3.1. The total internal energy ( $E_{\text{tot}}$  or  $E_i$ ) is the sum of all forms, including translational energy ( $E_{\text{tr}}$ ), rotational energy ( $E_{\text{rot}}$ ), vibrational energy ( $E_{\text{vib}}$ ), electronic energy ( $E_{\text{el}}$ ) and nuclear spin ( $E_{\text{sp}}$ ). The last two terms are negligible, so the  $E_{\text{tot}}$  is given by

$$E_{\text{tot}} = E_{\text{tr}} + E_{\text{rot}} + E_{\text{vib}} \quad 3.6.$$

At equilibrium, the ratio of molecules having energy  $E_i$  (energy at quantum state  $i$ ) to those having zero point energy (discussed in following section) is given by

$$\frac{n_i}{n_0} = g_i e^{-E_i/kT} \quad 3.7.$$

In equation 3.7,  $k$  is Boltzmann's constant ( $1.381 \times 10^{-23} \text{ J/K}$  or  $0.6951 \text{ cm}^{-1}\text{K}^{-1}$ ),  $T$  is temperature in K and  $g$  is a statistical term to account for possible degeneracy, or different states. The sum over all possible quantum states  $i$  accessible to the system is defined as the partition function  $Q$ , given by

$$Q = \sum g_i e^{-E_i/kT} \quad 3.8.$$

We can relate the partition function  $Q$  back to our equilibrium constant  $K$  (and ultimately our fractionation factor  $\alpha$ ) in equation 3.3 as

$$K = \frac{\prod (Q_i)^{n_i}_{\text{products}}}{\prod (Q_i)^{n_i}_{\text{reactants}}} = \frac{Q[\text{C}^{18}\text{O}][Q(^{16}\text{O}^{16}\text{O})]^{1/2}}{Q[\text{C}^{16}\text{O}][Q(^{18}\text{O}^{18}\text{O})]^{1/2}} \quad 3.9.$$

The total partition function  $Q_{\text{tot}}$  can be split up into the partition functions relating to the different forms of energy, translation, vibration and rotation,

$$Q_{\text{tot}} = Q_{\text{vib}}Q_{\text{rot}}Q_{\text{tr}} \quad 3.10.$$

The end result is that each of these components can be solved using quantum mechanics. The rotation and translation contributions for the different isotopologues are related only to mass difference. While the vibrational contribution to simple diatomic molecules is well known, the vibrations of atoms in complex multi-element compounds (especially solids and liquids) have contributions from interactions with multiple other atoms, and calculations become extremely complex. With accurate spectroscopic data, the fractionation between phases as a function of temperature can be computed. All that needs to be done is to compute the different components of the partition functions to determine our fractionation factors.

### 3.2.3 Vibrational Partition Function

We start by considering the potential energy of a diatomic molecule, such as H<sub>2</sub>. As a first approximation, the energy can be approximated as a simple harmonic oscillator, illustrated by the harmonic potential curve in Fig. 3.1. The two atoms will have an average distance between each other so as to minimize the energy. That is, they will tend towards the energy well in Fig. 3.1. If we bring two H atoms from far apart towards one another, there is an attraction. If they are moved too close to one another, repulsive forces overwhelm the attractive forces, and the atoms are pushed apart. The average spacing is at the base of the energy well. The energy for a harmonic oscillator is then given by

$$E = (n + \frac{1}{2})h\nu \quad 3.11$$

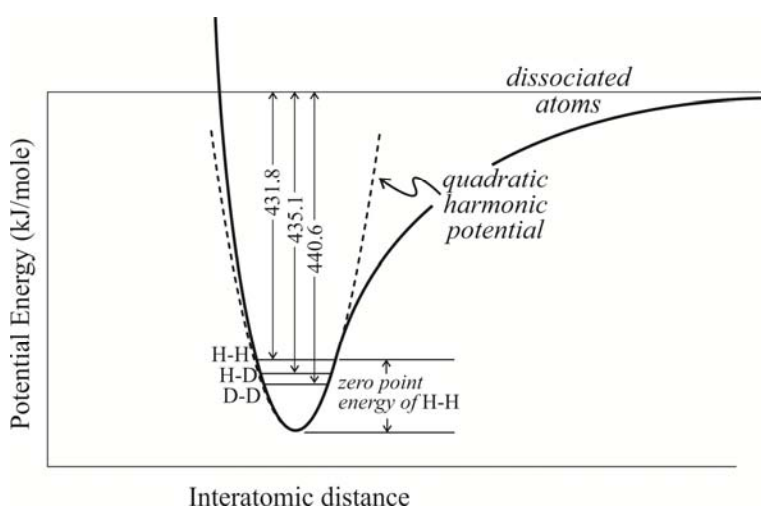


**Fig. 3.1.** Potential energy curve for diatomic hydrogen. Shown are the zero-point energies for the three isotopologues H-H, H-D, D-D. Note that D-D sits lower in the potential energy well than H-D or H-H and has a higher dissociation energy. The result is that the D-D bond is stronger than the H-H bond.

difference in their bond strengths. The amount of energy needed to dissociate a D-D molecule is larger than for an H-H molecule because the former resides lower in the potential well. More refined calculations of the vibrational energies take account of the deviation of the potential energy curve from the simple harmonic oscillator, but they will not be considered here.

where  $n$  is the vibrational energy level ( $n = 0, 1, 2$ , etc.),  $h =$  Planck's constant ( $6.626 \times 10^{-34}$  Jsec,  $\nu =$  frequency ( $\text{sec}^{-1}$ ). At low temperatures,  $n = 0$ , the ground vibrational state; at higher temperatures, higher energy levels are reached. But even at absolute zero, the vibrational energy is given by  $E = \frac{1}{2}h\nu$ , and the atoms move<sup>1</sup>. This is the **zero point energy**, given by the difference between the bottom of the potential energy well and the energy at the ground vibration state. The difference in the zero-point energy of H-H and D-D illustrates the

For a diatomic molecule a-b, the frequency  $\nu$  can be expressed by

<sup>1</sup> The atoms must move or they would violate the uncertainty principle, a fundamental law of quantum mechanics. If the atom had no motion, then we could tell exactly where it is and know its momentum, in violation of this law. . . something to do with a cat.

$$\nu = \frac{1}{2\pi} \sqrt{\frac{k_s}{\mu}} = \frac{1}{2\pi} \sqrt{k_s \left( \frac{1}{m_a} + \frac{1}{m_b} \right)} \quad 3.12.$$

Here,  $k_s$  is the effective spring constant (related to stiffness), and  $\mu$  is the reduced mass of molecule a-b ( $\mu = \frac{1}{\frac{1}{m_1} + \frac{1}{m_2}} = \frac{m_1 m_2}{m_1 + m_2}$ ). We can visualize this as two balls attached to

either end of a rigid spring. They vibrate towards and away from each other with the frequency  $\nu$ . When substituting the heavy isotope, the reduced mass changes, but the spring constant is unchanged. Imagining our two-ball model, the frequency is reduced due to substitution by the heavier mass – the balls vibrate more slowly.  $\nu$  is related to the wave number  $\omega$  by  $\nu = \omega c$ , where  $c$  is the speed of light ( $2.998 \times 10^{10}$  cm/sec). Wave numbers are measured from spectroscopic data, or for our purposes, taken from published tabulations. For  $^{12}\text{C}^{16}\text{O}$ ,  $\omega = 2167.4 \text{ cm}^{-1}$ , and the spring constant (from 3.12 above) is easily calculated (see problem 5). The wave number for  $^{12}\text{C}^{18}\text{O}$  is simply given by the relationship

$$\frac{\nu^*}{\nu} = \sqrt{\frac{\mu}{\mu^*}} \quad 3.13$$

where the \* refers to the isotopically substituted molecule. The frequency of  $^{12}\text{C}^{18}\text{O}$  is calculated to be  $2115.2 \text{ cm}^{-1}$ .

If we consider the simple harmonic oscillator equation 3.8 becomes

$$Q_{vib} = \sum_i e^{-E_{vib}/kT} = \sum_{n=0}^{\infty} e^{-(n+1/2)hv/kT} \quad 3.14.$$

Separating the terms, 3.14 is given by

$$Q_{vib} = e^{-U/2} \sum_{n=0}^{\infty} e^{-(n)U} \quad 3.15$$

where  $U = \frac{hv}{kT} = \frac{hc\omega}{kT}$ . The following approximation can be applied (Criss, 1999):

$$\sum_{n=0}^{\infty} x^n = \frac{1}{1-x} \quad (\text{for } 0 < x < 1) \quad 3.16,$$

such that

$$Q_{vib} = e^{-U/2} \frac{1}{1 - e^{-U}} \quad 3.17.$$

The  $E_{vib}$  values for  $C^{16}O$  and  $C^{18}O$  are  $2.1527 \times 10^{-20}$  J/mole and  $2.10084 \times 10^{-20}$  J/mole (from Equation 3.11). The ratio  $Q_{vib}(C^{18}O)/Q_{vib}(C^{16}O)$ , called **the vibrational partition function ratio**, is 1.1343, which we will return to in equation 3.20.

### 3.2.4 Translational and Rotational Partition Function

The translational partition function ratio is dependent on a number of terms, but ultimately, the translational partition function ratio of a diatomic molecule with different masses simplifies to

$$\frac{Q_{2tr}}{Q_{1tr}} = \left( \frac{M_2}{M_1} \right)^{3/2} \quad 3.18.$$

Here  $M_1$  and  $M_2$  are the molecular masses of the two molecules. Note that it is independent of temperature.

The rotational partition function is also a function of a number of terms which cancel out when we take the ratio of the two isotopically-substituted molecules. For a diatomic molecule, the rotational partition function ratio is given by

$$\frac{Q_{2rot}}{Q_{1rot}} = \frac{\sigma_1 I_2}{\sigma_2 I_1} \quad 3.19,$$

where  $\sigma$  is the symmetry number, and  $I$  is the moment of inertia. For CO, where only one molecule is exchanged,  $\sigma = 1$ . For  $O_2$ , where  $^{18}O$  can occupy one of two sites,  $\sigma = 2$ .  $I = \mu r^2$ , where  $\mu$  is the reduced mass, and  $r$  is the average interatomic distance.

### 3.2.5 The complete Partition Function Ratio

Combining all partition function ratios into one complete term gives

$$\frac{Q_2}{Q_1} = \left( \frac{M_2}{M_1} \right)^{3/2} \frac{\sigma_1 I_2}{\sigma_2 I_1} \frac{e^{-U^*/2}}{e^{-U/2}} \frac{1 - e^{-U}}{1 - e^{-U^*}} \quad 3.20$$

( $U^*$  is the isotopically substituted species). The above equation can be simplified using the Teller-Redlich spectroscopic theorem (see O'Neil, 1986, page 9) to give a final solution

$$\frac{Q_2}{Q_1} = \left( \frac{m_2}{m_1} \right)^{3/2} \frac{\sigma_1 \bar{\omega}_2}{\sigma_2 \bar{\omega}_1} \frac{e^{-U^*/2}}{e^{-U/2}} \frac{1 - e^{-U}}{1 - e^{-U^*}} \quad 3.21$$

Here,  $m$  is atomic mass, and this term will cancel out, as will the term  $\sigma_1/\sigma_2$ . For  $C^{16}O$ - $C^{18}O$ , we have the following:  $\omega_2/\omega_1 = 0.9759$ , and  $\frac{e^{-U^*/2}}{e^{-U/2}} = 1.134$ , ( $\frac{1-e^{-U}}{1-e^{-U^*}} = 1$ ) giving

the total partition function ratio of 1.1069. A similar calculation for  $O_2$  gives a partition function ratio of 1.08304. Partition function ratios can be divided by one another to give respective  $\alpha$  values. The  $\alpha_{CO-O_2}$  is therefore  $1.1069/1.08304 = 1.022$  at 25 °C.

### 3.2.6 Extension to more complex molecules

Polyatomic gases, and solids can be treated in a similar manner to the above sets of equations, treating all possible modes of vibration in the summation terms. A number of assumptions and simplifications need to be made because the quantum states of molecules in liquids and solids (and high pressure gases) are not independent from each other. Extensions of the above models have been considered by a number of authors for relatively simple phases such as calcite, quartz, and  $UO_2$  (e.g., Bottinga, 1968; Hattori and Halas, 1982). Kieffer (1982) made some simplifying assumptions and was able to predict relative isotopic enrichments of more complex minerals. The largest uncertainty in calculating partition function ratios for complex solids is estimating the frequency shifts for the isotopically-substituted molecule. Schauble (2004, and references therein) has predicted stable isotope fractionation for some elements other than those in the H-C-N-O-S system. Polyakov and Mineev (2000) used Mössbauer spectroscopy for estimating isotopic fractionation, and Driesner and Seward (2000) made simulations of salt effects on liquid-vapor partitioning.

### 3.2.7 'Empirical' theoretical methods

Several methods of determining fractionation factors have been developed that take advantage of the empirical relationship between bond strength and relative isotope enrichment (Schütze, 1980; Richter and Hoernes, 1988; Smyth, 1989; Zheng, 1993; Hoffbauer et al., 1994). These techniques are based on ordering minerals according to their increasing anionic bond strength. Smyth's method involved calculating electrostatic site potentials for anionic sites, a function related to the bond strength of the oxygen in different crystallographic locations. Variations on this method include consideration of the effects of cation site and coordination. These latter methods are called 'the increment method'. They require that the relative bond strength data be calibrated to some independently (experimentally or theoretically) determined oxygen isotope fractionation relationship and then the correlations are extended to the entire data set. The general enrichment obtained with this method is mostly consistent with experimental data, but there are a number of notable exceptions, such as an overemphasis of polymorphic substitution (e.g., Sharp, 1995). The major advantage of the technique is that it can be applied to almost any mineral, is 'internally consistent' and is easy to use. As a result, the increment method has been widely embraced. It should be pointed out, however, that these methods are not based on any known physical or chemical laws relating isotope fractionation to anionic bond strengths, and they should be used with caution, as their results sometimes are in serious disagreement with other calibrations.

Savin and Lee (1988) devised an empirical bond-type approach for determining fractionation factors for phyllosilicates, particularly clay-forming minerals. They assume

that oxygen in a given chemical bond has similar isotopic fractionation behavior regardless of the mineral in which it is located. Once fractionations are assigned to each bond type (e.g., Si-O-Si, Al-O-Si, Al-OH, etc.), the fractionation for the entire mineral can be determined by summing the proportions of each bond. In general, the agreement between their method and experimental and empirical calibrations is good. In the case of low-temperature clay minerals, such methods are necessary, because experimental data are limited by the sluggish reaction rates of minerals in low-temperature range defining their stability field and the structures are too complex to treat using statistical mechanics.

### 3.3 Relationship to temperature

Bigeleisen and Mayer (1947) derived the following expression for partition function ratios:

$$\frac{Q_2}{Q_1} = 1 + \left( \frac{1}{2} + \frac{1}{U_2} + \frac{1}{e^{U_2} - 1} \right) \Delta U \quad 3.22.$$

$U_i = \frac{hc\bar{\omega}_i}{kT}$ , and  $\Delta U$  is  $U_1 - U_2$ . If  $U$  is large, then  $\frac{Q_2}{Q_1} \approx 1 + \frac{1}{2}\Delta U$ . This would be the case when vibrational frequencies are high (such as reactions involving hydroxyl groups or water) or temperature are low. Under such conditions,  $\frac{Q_2}{Q_1}$  is clearly proportional to  $1/T$ .

When  $U$  is less than 5, the terms in parentheses approaches a value of  $U/12$ . In this case,  $\frac{Q_2}{Q_1}$  will be proportional to  $1/T^2$ . At room temperature and above, for anhydrous minerals (where wave numbers are less than  $1000 \text{ cm}^{-1}$ ), the  $1/T^2$  relationship holds. As a result, the fractionation between phases  $m$  and  $n$  is defined as

$$1000 \ln \alpha_{m-n} = \frac{a \times 10^6}{T^2} + b \quad (\text{T in K}) \quad 3.23$$

at high temperatures and

$$1000 \ln \alpha_{m-n} = \frac{a \times 10^6}{T} + b \quad (\text{T in K}) \quad 3.24$$

at low temperatures, where  $a$  and  $b$  are constants. The temperature at which the crossover between 3.24 and 3.23 occurs is not known, but is probably below room temperature for most phases as discussed in section 3.2.7.

At infinite temperatures, the fractionation between any two phases approaches 0‰. Yet from equation 3.23, at  $T = \infty$ ,  $1000 \ln \alpha = b$ , which is clearly not correct. The  $b$  term cannot be constant over the complete temperature interval and must approach 0 at extremely high temperatures. Fractionation equations using both a  $1/T^2$  and  $1/T$  have been used (Zheng, 1993) as well as polynomials of  $1/T^2$  such as (Clayton and Kieffer, 1991)

$$1000 \ln \alpha_{m-n} = a \left( \frac{10^6}{T^2} \right) + b \left( \frac{10^6}{T^2} \right)^2 + c \left( \frac{10^6}{T^2} \right)^3 \dots \quad 3.25.$$

Bottinga and Javoy (1973) argued that equation 3.23 applies to all rocks. The  $b$  constant is 0 for fractionation between anhydrous phases, phases for which the vibrational frequencies vary from 900 to 1200 cm<sup>-1</sup>. For water, the vibrational frequencies are far higher, ranging from  $\omega_2 = 1647$  to  $\omega_3 = 3939$  cm<sup>-1</sup>. Fractionation between an anhydrous mineral and water will have a  $b$  term = 3.7<sup>2</sup>. Finally, for fractionation between anhydrous minerals and hydrous minerals, the  $b$  term is proportional to the number of OH bonds in the phase. Others have questioned the validity of this term when applied to solid-solid equilibria (e.g., Chacko et al., 1996).

### 3.4 Experimental determination of fractionation factors

#### 3.4.1 Introduction

The first application of stable isotope thermometry was to the calcite-water system. McCrea (1950) synthesized calcite in water at room temperature and also estimated fractionation factors between calcite and water using statistical mechanical methods. Epstein *et al.* (1951; 1953) were able to determine the apparent equilibrium calcite-water fractionation at 29 and 31°C by drilling small holes into living snails and bivalves (*Pinna* sp.). The organisms repaired their shells in an aquarium held at constant temperature where the  $\delta^{18}\text{O}$  value of ambient water was held to a constant and known value. The newly-repaired material was removed and analyzed in order to determine the calcite-water fractionation at those specific temperatures (see section 6.3 for a more detailed discussion of carbonate-water fractionation).

More commonly, experiments are made by synthesizing or equilibrating two phases at high temperatures. O'Neil *et al.* (1969) expanded on McCrea's earlier work, both by synthesizing calcite at room temperature conditions and by equilibrating calcite and water at high temperatures in hydrothermal bombs. Their results agreed with the earlier low-temperature calibration of Epstein's earlier work using shells.

All high-temperature experiments are made by isotopically equilibrating two phases. There are several issues that must be overcome for a successful calibration:

- 1) Isotopic equilibrium must be achieved, or at least a quantification of the degree of equilibration must be known.
- 2) The phases must be separable for isotopic analysis. Fine grained intergrowths of two silicate minerals may be inseparable for traditional bulk analysis and therefore not amenable to the experimental technique.

The first of these concerns is met by employing one of several strategies. Commonly, starting materials are extremely fine-grained. Many experimental papers describe 'floating the minerals on acetone' which results in micron-size particles. During the subsequent heating experiment, grains recrystallize and grow. During this process,

---

<sup>2</sup> The value of 3.7 was determined from averaging data from experimental studies. See original paper for details.

oxygen exchange occurs as a result of the bond breaking and reforming. Other strategies include using metastable starting materials (such as silica gel which recrystallizes to quartz during prolonged heating) or equilibrating a mineral in a fluid that is not in chemical equilibrium with the starting material. For example, O'Neil and Taylor (1967) reacted sodium feldspars with a KCl solution. In the course of the analysis, the cations exchanged so that by the end of the reaction, the sodium feldspar had been converted to potassium feldspar. The high free energy of the cation exchange reaction was found to drive oxygen bond breaking so that oxygen isotope equilibration between the fluid and mineral would occur.

The use of fine-grained starting materials leads to the second problem. If the run products consist of intimately intergrown minerals, separation for bulk isotope analysis can be virtually impossible. Partly for this reason, most exchange experiments have been made with water or more rarely CO<sub>2</sub> gas, so that there is only one solid phase. Clayton *et al.* (1989) developed a calcite-mineral exchange technique, where at high pressure and temperature, recrystallization led to a high degree of oxygen isotope exchange. The calcite could then be easily separated from the silicate by reaction with phosphoric acid – the typical method for analyzing carbonates. Oftentimes, an experimental calibration may not be of geological interest – for example albitie-CO<sub>2</sub> gas fractionations – but the combination of two experiments can give a third fractionation that is geologically relevant. Consider the following example. Experimental fractionation factors have been measured for quartz-water and muscovite-water. Combining the results of these experiments gives the important quartz-muscovite equation, a widely-used isotope thermometer. Quite simply, the *a* and *b* terms can be subtracted from one another to eliminate the intermediate phase:

$$\begin{array}{l} \text{If} \quad 1000\ln\alpha(\text{qz-water}) = 4.10 \times 10^6/T^2 - 3.70 \\ \text{and} \quad 1000\ln\alpha(\text{musc-water}) = 1.90 \times 10^6/T^2 - 3.10, \\ \text{then} \quad 1000\ln\alpha(\text{qz-musc}) = 2.20 \times 10^6/T^2 - 0.6. \end{array}$$

The choice of exchange medium (water, calcite, CO<sub>2</sub>) is determined on the basis of a number of factors. Each has advantages and disadvantages as discussed below.

### 3.4.2 Mineral-water exchange reactions

Most early exchange experiments were made for mineral-water pairs. 10 to 20 mg. of a finely-ground solid, and ~200 mg. of water are sealed in a noble-metal tube and heated to reaction temperature at a confining pressure of 1-2 kbar<sup>3</sup>. The experiments are relatively easy to perform, reaction rates are moderately rapid, and the initial isotopic composition of the water starting material can be varied.

In order to test for equilibrium, mineral-water exchange reactions are made by starting with waters that have  $\delta$  values both higher and lower than the presumed equilibrium value. In this way, the equilibrium fractionation is approached from both directions (Fig. 3.2). Because the rates of reaction are independent of the direction of

---

<sup>3</sup> Some experiments have been made in piston-cylinder apparatus at much higher pressures, with smaller sample charges. Although more difficult, exchange rates are generally enhanced (Matthews *et al.*, 1983), and certain mineral stability fields may be extended to higher temperatures at high pressures.

approach, the results can be extrapolated to infinite time to find the exact equilibrium value<sup>4</sup>.

In theory, experiments need be made only at a single temperature. From equation 3.23, the  $a$  constant can be determined (assuming  $b = 3.7$ ) and extended over the entire temperature range. In practice, experiments are made at a series of temperatures, and the best-fit line through the data are used to calculate both  $a$  and  $b$  (Fig. 3.3).

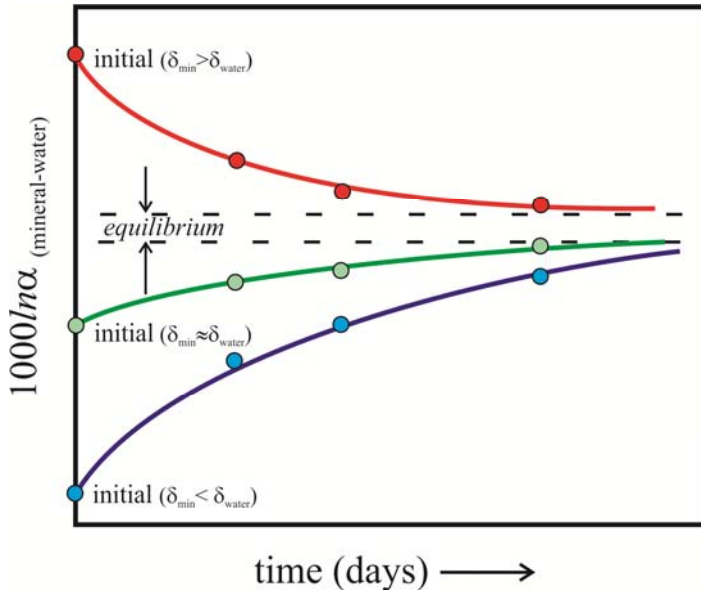


**Fig. 3.2.** Schematic of progressive degrees of isotopic exchange between a mineral and water as a function of time. Experiments are made with waters of different initial isotopic compositions. Multiple capsules can be put into a high P-T charge together and the different experiments all approach a single  $1000 \ln \alpha$  value with increasing time.

temperatures, fractionations between the mineral and water become very small, so that the uncertainties in the measurements become an important problem. The general solution is to run the fractionation experiments over a range of temperatures and fit the data to the appropriate equations (Fig. 3.3). Nevertheless, as numerous authors have discussed, it is impossible to know if the recrystallization-based exchange is actually being driven towards the equilibrium value. Recrystallization is the thermodynamic driving force in these hydrothermal exchange experiments and it is not clear that isotopic equilibrium follows the recrystallization.

There are several important considerations regarding the mineral-water experimental method. First, there are both low and high temperature limits on exchange experiments. If the temperatures are too low, reaction kinetics are too sluggish and little exchange occurs. If the reactions are run at temperatures that are very high, then significant dissolution of the solid (*e.g.*, quartz) will occur into the fluid phase. During subsequent quench, the dissolved phase will rapidly precipitate, causing disequilibrium. The dissolved species may even have a different fractionation with water than the equivalent crystal. At very high

<sup>4</sup> See Northrop and Clayton (1966) and O'Neil (1986) for the mathematical treatment of this approach.

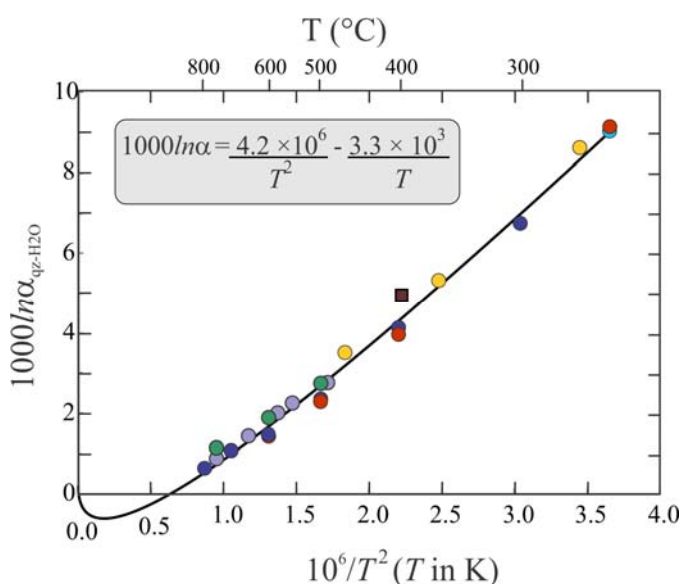


**Fig. 3.3.** Best fit line of equation  $1000 \ln \alpha = a/T^2 + b/T$  to published quartz-water exchange experiment data. The studies were made using different techniques and yet still give similar results. The negative  $1/T$  term results in a best-fit that has a reversal in the  $1000 \ln T$  value at high temperatures, a result that is consistent with many mineral-water fractionation studies. The square symbol is a combination of  $\text{CO}_2$ -silica and  $\text{CO}_2$ - $\text{H}_2\text{O}$  fractionations. Modified from (Sharp et al., 2016).

water, and the  $b$  term in equation 3.23 reduces to 0. Also dissolution in aqueous solutions and recrystallization during quench are eliminated.

There are several drawbacks to this method as well. It is clear that at all but the highest temperatures, isotopic equilibration occurs only because the solids undergo recrystallization. Like the mineral-water experiments, the driving force towards equilibrium is recrystallization, and there is no way to know if the changes in stable isotope ratios are trending towards the equilibrium values or are controlled by kinetically based recrystallization. A second limitation is that exchange rates are far slower than for the mineral-water system. This raises the lower-limits on the temperatures at which significant exchange occurs, and hence reduces the possible temperature range of calibration.

#### 3.4.4 Mineral- $\text{CO}_2$ exchange reactions

The idea of measuring the fractionation between a solid and  $\text{CO}_2$  gas was pioneered by O'Neil and Epstein (1966) and resurrected over two decades later (Chacko et al., 1991; Stolper and Epstein, 1991). Mineral- $\text{CO}_2$  exchange has the distinct advantage over other experimental methods in that, except at high very high temperatures and pressure (Chacko et al., 1991), no recrystallization of the solid phases occurs during the reaction. Exchange should be purely diffusional in nature, and therefore tend towards equilibrium. The experimental setup is simple as well. Finely powdered samples are

#### 3.4.3 Mineral-calcite exchange reactions

Clayton *et al.* (1989) developed a new method for high pressure exchange experiments using calcite as the exchange medium. Starting materials were finely admixed calcite and mineral. During the course of the experiment, recrystallization occurred and there was presumably an approach towards isotopic equilibrium. The novel method, which has since been employed for a number of minerals, has two striking advantages over earlier experiments, but several potential problems as well.

The main advantage, of course, is that water is eliminated as a reactant. This removes the complication from the high O-H stretching frequencies characteristic of

loaded in silica or metal tubes, CO<sub>2</sub> is introduced and the tube is sealed. After heating, the  $\delta^{18}\text{O}$  value of the CO<sub>2</sub> is measured, which should be in equilibrium with the solid phase. Combining the experimental CO<sub>2</sub>-silica (Stolper and Epstein, 1991) and theoretical CO<sub>2</sub>-H<sub>2</sub>O (Richet et al., 1977) fractionations gives a silica-water fractionation only slightly higher than the quartz-H<sub>2</sub>O fractionations (Fig. 3.3).

The major limitation of this type of experiment is that exchange is very slow. Only phases that have very high oxygen diffusion rates, such as carbonates, albite, and silica glass, are accessible to this approach.

#### 3.4.5 The three-phase approach

Several studies have used both calcite and water ( $\pm\text{CO}_2$ ) as the exchange medium (Zheng et al., 1994b; Hu and Clayton, 2003). With judicious proportions of H<sub>2</sub>O and CO<sub>2</sub>, exchange experiments for mineral phases that would otherwise be unstable (e.g., hydrous phases, Zheng et al., 1994a) can be made. The presence of water also enhances reaction rates between the mineral and carbonate.

### 3.5 Empirical determination of fractionation factors

Empirical determinations are made by measuring the fractionation between two natural phases with temperatures either measured (for modern samples) or calculated (for example, when using metamorphic rocks). Some of the most successful, low temperature calibrations have been made using empirical calibrations, notably the calcite-water (Epstein et al., 1953), phosphate-water (Longinelli and Nuti, 1973), and silica-water (Leclerc and Labeyrie, 1987) systems. The isotopic composition of shells (or diatoms for silica) and coexisting water were measured, and then compared to measured temperatures of growth. The original (calcite, phosphate, silica) - water equations have withstood the test of time with very little modification.

Other low temperature equations have been made for clay minerals, where temperatures of formation are estimated from the depositional environment. Savin and Epstein (1970) estimated the oxygen and hydrogen isotope fractionation for kaolinite-water, montmorillonite-water and glauconite-water at low temperature. Other low temperature examples include gibbsite (Bird et al., 1994), and silica (Leclerc and Labeyrie, 1987). These empirical studies are particularly successful because exchange experiments are virtually impossible at room temperature; the only experimental avenue to low temperature exchange is mineral synthesis.

Modern empirical estimates have also been made at higher temperatures, often taking advantage of unique and unusual conditions. Amorphous silica-water fractionation was determined from deposits of thermal waters from power plants (Kita et al., 1985) and quartz-water, calcite-water and adularia-water fractionations were measured from the Broadlands geothermal field, New Zealand in drill cores where water could be samples and temperatures measured (Blattner, 1975).

Finally, fractionation factors have been made from minerals in metamorphic or igneous rocks where independent temperature estimates are available. In some cases, empirical estimates are the only option available to the isotope geochemist. For certain

'refractory' phases<sup>5</sup>, the experimental approach is limited due to extremely sluggish reaction rates, so that empirical estimates are our only option. A good example is for the quartz-aluminum silicate system, where empirical estimates have been applied to a number of metamorphic terranes (Sharp, 1995). The effect of complex chemical substitutions can also be estimated from natural assemblages (Taylor and O'Neil, 1977; Kohn and Valley, 1998), bypassing the huge effort that would be required to make such measurements experimentally. In all cases, multiple samples from multiple localities should be analyzed to avoid any problems that might inadvertently exist within a single, potentially 'anomalous' site. Consider the case of trying to determine the equilibrium fractionation between orthopyroxene and clinopyroxene from mantle xenoliths. The minerals equilibrated at high temperatures, over an inordinately long time period, and cooled rapidly following eruption. A perfect natural laboratory. And yet we find that in some xenoliths, the clinopyroxene has a higher  $\delta^{18}\text{O}$  value than coexisting orthopyroxene, and in other samples it is reversed (Perkins et al., 2004). Clearly empirical estimates should not be made by analyzing a single rock, with the thought that the results are universally applicable.

There are a number of advantages to making empirical estimates. First and foremost, the amount of time that a mineral has had to reach equilibrium with its surrounding far exceeds anything that could be accomplished in the laboratory. A metamorphic rock heated to 500°C for millions of years provides a nice contrast to the same system heated to 900°C in the laboratory for a period of hours or days. Also, many of the potential pitfalls inherent in experimental studies, such as quench recrystallization, metastable equilibria, and difficulty of separating fine-grained materials can be avoided by measuring natural materials.

As with all calibration methods, numerous concerns exist as well. The most serious of these are 1) knowing the precise temperature at which equilibrium was attained, 2) that the minerals of interest were indeed in equilibrium and did not 'inherit' their isotopic composition from an earlier metamorphic event and 3) insuring that no retrograde exchange occurred during cooling. This is particularly a concern for slowly-cooled metamorphic rocks, where some diffusional resetting is expected. The problem is illustrated when considering the  $\Delta^{18}\text{O}$  (quartz-feldspar) values commonly measured in igneous rocks (Chapter 11). Fractionations commonly range from 1.5 to 2.5‰, corresponding to temperatures of 430-640°C, clearly lower than the crystallization temperature of the granite, indicating that post-crystallization isotopic exchange occurred.

### 3.6 Other factors controlling isotope partitioning

#### 3.6.1 Pressure effect

The effect of pressure on the equilibrium constant is given by

$$\left(\frac{\partial \ln K}{\partial P}\right)_T = -\frac{\Delta V_R}{RT} \quad 3.26,$$

---

<sup>5</sup> Minerals fitting into this category include kyanite, garnet, zircon, corundum, and staurolite for oxygen and certainly diamond and graphite for carbon.

where  $\Delta V_R$  is the volume change of the reaction. For an isotope exchange reaction such as Equation 3.1, the  $\Delta V_R$  term is close to zero, so that pressure will have a minimal effect on the fractionation between coexisting species. Hoering (1961) first demonstrated the insensitivity of fractionation to pressure when he measured the  $^{16}\text{O}/^{18}\text{O}$  fractionation between  $\text{H}_2\text{O}$  and  $\text{HCO}_3^-$  at 1 atmosphere and at 4 kilobars (both at  $43.5^\circ\text{C}$ ). There was a change of  $0.2 (\pm 0.2) \text{‰}$  fractionation between 4 kb and 1 atm, which he concluded was negligible. Later, calcite-water and quartz-water exchange experiments were made

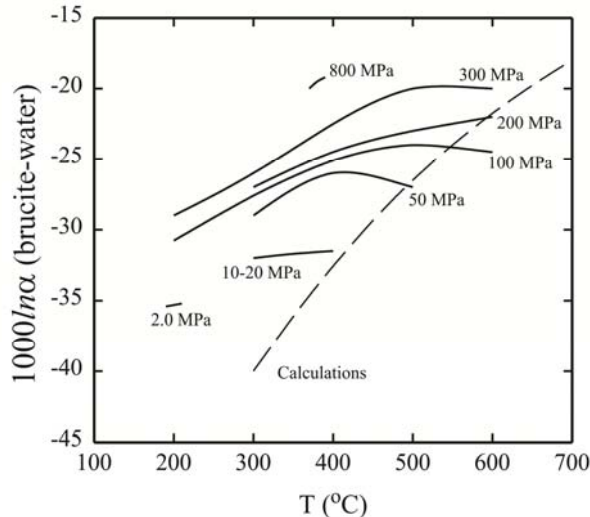


**Fig. 3.4.** Hydrogen isotope fractionation between brucite and water as a function of temperature for various pressures. The dashed line labeled ‘Calculations’ is the theoretical fractionation between brucite and water at 1 bar, based on statistical mechanical calculations. With increasing pressures there is an increase in brucite-water fractionations; the effect decreases with increasing temperature. From (Horita *et al.*, 2002). Used with permission.

over a pressure range of 1 to 20 kbar, with no detectable pressure effect (Clayton *et al.*, 1975; Matthews *et al.*, 1983). Polyakov and Kharlashina (1994) devised a statistical mechanical method of estimating pressure effects. For most rocks exposed at the Earth’s surface, the pressure effect will be near the detection limits of analysis. At very high pressures, however, the effects can be significant. Using the Polyakov and Kharlashina method, Sharp *et al.* (1992) found that quartz is particularly sensitive to pressure. For most minerals, the electrostatic site potentials increase slightly with pressure, but the reverse is found for quartz. As a result,  $\Delta^{18}\text{O}_{\text{qz-min}}$  values will change by  $\sim 0.5 \text{‰}$  at  $1200^\circ\text{C}$  and 40 kbar. Fortunately, the unusual behavior of quartz becomes redundant because coesite is the stable  $\text{SiO}_2$  polymorph above  $\sim 27$  kbar.

The effect of pressure is larger for graphite-diamond (Polyakov and

### 3.6.2 Oxidation state

But the really striking pressure effects are seen for D/H fractionation between hydrous minerals and water. Fig. 3.4 shows the effect of pressure on the brucite-water fractionation as a function of pressure and temperature. In their combined experimental-theoretical study, Horita *et al.* (2002) conclude that water is much more strongly affected than hydrous minerals, so that hydrogen isotope fractionation pressure effects should exist for all water - hydrous mineral pairs.

The largest effect on fractionation is oxidation state. The  $1000 \ln \alpha$  value (at  $20^\circ\text{C}$ ) for carbon in the  $\text{C}^{4+}$  ( $\text{CO}_2$ ) vs  $\text{C}^4$  ( $\text{CH}_4$ ), for sulfur in the  $\text{S}^{6+}$  ( $\text{SO}_3$ ) vs  $\text{S}^{2-}$  ( $\text{H}_2\text{S}$ ) and for chlorine in the  $\text{Cl}^{7+}$  ( $\text{ClO}_4^-$ ) vs  $\text{Cl}^-$  are all around 70‰. This explains why biological redox reactions have such large isotopic fractionations as evidenced by reduction of sulfate to sulfide and  $\text{CO}_2$  to methane. The theoretical fractionations for hydrogen far outweigh any

other element. The calculated  $1000\ln\alpha$  value for H<sub>2</sub>O and H<sub>2</sub> at 20°C is over 1000‰ (Richet et al., 1977).

Oxygen has one oxidation state and so is not affected by the redox changes that occur in most of the other elements used for stable isotope studies. The heavy isotope of oxygen will be preferentially fractionated into short, strong chemical bonds (such as Si<sup>4+</sup>) generally with a high oxidation state. Note however that uraninite (U<sup>4+</sup>O<sub>2</sub>) strongly incorporates <sup>16</sup>O relative to quartz, so that oxidation state alone does not always correlate with oxygen isotope enrichment.

### 3.6.3 Composition

Taylor and Epstein (1962) devised a simple relationship between composition and isotopic enrichment, recognizing that bond strength – and oxygen isotope enrichment – decrease from Si-O bonds through Al-O to M<sup>2+</sup>-O = M<sup>1+</sup>-O bonds. Minerals follow this rule quite well and it should be kept in mind as a qualitative guide to oxygen isotope enrichment in rocks. Quartz almost always has the highest δ<sup>18</sup>O value, followed by feldspar and continuing down to the Si- and Al-free oxides such as magnetite, rutile and hematite. Rough estimates of relative isotopic enrichment are easily made by keeping this rule in mind. Consider olivine and clinopyroxene. Which one will concentrate <sup>18</sup>O relative to the other? Mg<sub>2</sub>SiO<sub>4</sub> has a lower proportion of Si-O bonds than MgSiO<sub>3</sub> (or CaMgSi<sub>2</sub>O<sub>6</sub>), and consequently a lower δ<sup>18</sup>O value. In general, substitution of identically-charged cations (*e.g.*, Na ↔ K, Fe ↔ Mg, Ca ↔ Mn) has a minimal effect on isotopic fractionation<sup>6</sup>. There is no oxygen isotope fractionation between albite and potassium feldspar (NaAlSi<sub>3</sub>O<sub>8</sub> vs. KAlSi<sub>3</sub>O<sub>8</sub>), nor between almandine and pyrope (Fe<sub>3</sub>Al<sub>2</sub>Si<sub>3</sub>O<sub>12</sub> vs. Mg<sub>3</sub>Al<sub>2</sub>Si<sub>3</sub>O<sub>12</sub>), and only a small effect of Ca ↔ (Mg, Fe) substitution.

A much larger fractionation exists for coupled substitutions, such as NaSi ↔ CaAl in plagioclase (NaAlSi<sub>3</sub>O<sub>8</sub> ↔ CaAl<sub>2</sub>Si<sub>2</sub>O<sub>8</sub>), and NaAl ↔ Ca(Mg,Fe) in pyroxene (NaAlSi<sub>2</sub>O<sub>6</sub> ↔ CaMgSi<sub>2</sub>O<sub>6</sub>). The temperature coefficient of fractionation (*a* term in equation 3.23) is 0.94 for quartz-albite, increasing by 1.05*x* (*x* = fraction of anorthite in plagioclase) up to 1.99 for pure anorthite. Other substitutions that affect isotopic fractionation are F ↔ OH in phlogopite and Al<sup>3+</sup> ↔ Fe<sup>3+</sup> in garnet. See Chacko *et al* (2001a) for more details.

The effect of composition on hydrogen isotope fractionation has not been thoroughly studied, but in a seminal paper on the subject, Suzuoki and Epstein (1976) found that Al has the strongest affinity for deuterium, followed by Mg and Fe. They proposed a general equation to predict hydrogen isotope exchange between hydrous minerals and water given by<sup>7</sup>

$$1000\ln\alpha_{\text{mineral-H}_2\text{O}} = \frac{-22.4 \times 10^6}{T^2} + 26.3 + (2X_{\text{Al}} - 4X_{\text{Mg}} - 68X_{\text{Fe}}) \quad 3.27,$$

<sup>6</sup> Note that Fe has a strong effect of H isotope fractionation (see equation 3.27).

<sup>7</sup> Equation 3.26 contained a printing error in the original publication. The constant 26.3 was originally given as 28.2 (Morikiyo, 1986).

where X refers to the portion of each element in the octahedral site. The above equation generally predicts the correct degree of enrichment, but not necessarily the correct temperature dependence (Chacko et al., 2001a).

### 3.6.4 Salinity

There is a great deal of confusion about the effect of salinity on the isotope fractionation between water and coexisting phases. Many authors refer to 'the salinity effect' when discussing the carbonate-water paleothermometer. Unfortunately, many practitioners mistakenly assume that the addition of dissolved cations changes the oxygen isotope fractionation between calcite and water. The 'salinity effect', as discussed in Chapter 6, is actually related to the loose correlation between salinity and the degree of freshwater contamination (and hence lowering of the  $\delta^{18}\text{O}$  value) in the ocean.

The actual effects of salinity are variable both for different dissolved salts and as a function of temperature. The fractionation between a salt solution and pure water varies linearly with molality and has a large positive value for salts with a high degree of 'structure making' electrolytes, and a negative fractionation for salts with 'structure-breaking' electrolytes (O'Neil and Truesdell, 1991), roughly correlating to cation charge

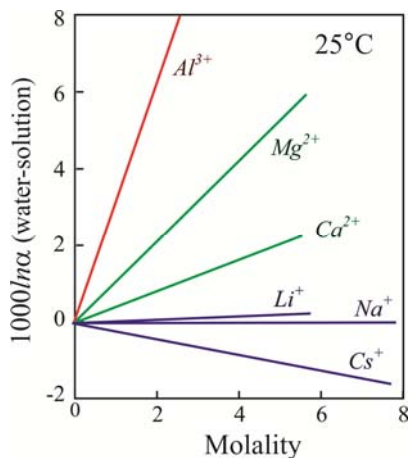


**Fig. 3.5.** The fractionation of dissolved salt solutions relative to pure water. Modified from (O'Neil and Truesdell, 1991)

(Fig. 3.5). Importantly, the effect of salinity (mostly related to dissolved NaCl) on the ocean has a completely negligible effect on the equilibrium fractionation between  $\text{H}_2\text{O}$  and authigenic minerals (*e.g.*, calcite). For all but concentrated  $(\text{Ca},\text{Mg})\text{Cl}_2$  and  $\text{MgSO}_4$  solutions, however, the effects for both hydrogen and oxygen can be ignored at low temperature. At temperatures above  $200^\circ\text{C}$ , a concentrated NaCl solution is enriched in the heavy isotope relative to pure water (Driesner and Seward, 2000). Studies of salt effects are extremely useful in understanding the solvation of dissolved cations in aqueous solutions.

An elegant set of experiments on hydrogen and oxygen isotope salt effects was made in a series of papers by Horita *et al.* (Horita et al., 1993a; Horita et al., 1993b; Horita et al., 1995) and should be consulted for further information.

### 3.6.4 Polymorphism

The effect of polymorphism generally has a 'second-order' effect on fractionation. unimportant for the most part. For example, no oxygen isotope fractionations have been seen between the different aluminum silicate polymorphs andalusite, kyanite, and sillimanite, where coexisting polymorphs are found to have nearly identical  $\delta^{18}\text{O}$  values (Cavosie et al., 2002; Larson and Sharp, 2003). There are several notable exceptions, where a polymorphic transition has a significant isotope effect, including graphite-diamond (Bottinga, 1969), calcite-aragonite (oxygen, Rubinson and Clayton, 1969), and perhaps quartz and coesite. For most polymorphic transitions, the effects are negligible.

### 3.7 Multiple isotope system: The “Big Δ” notation

Oxygen and sulfur have three and four stable isotopes, respectively. Many of the non-traditional isotope systems also have multiple isotopes (Sn has the record with 10!). The early practitioners of stable isotope geochemistry recognized that there were fundamental mass dependent fractionation processes that appeared to make measurements of the rare isotopes redundant. For example, Craig (1957) noted the following relationship between  $^{17}\text{O}/^{16}\text{O}$  and  $^{18}\text{O}/^{16}\text{O}$ :

$$\left( \frac{R^{18}_{\text{sample}}}{R^{18}_{\text{standard}}} \right)^{\lambda} = \left( \frac{R^{17}_{\text{sample}}}{R^{17}_{\text{standard}}} \right) \quad 3.28,$$

where  $R^x =$  is the  $^x\text{O}/^{16}\text{O}$  ratio and  $\lambda$  (for oxygen) is close to 1/2. This means that the  $\delta^{17}\text{O}$  value is related to the  $\delta^{18}\text{O}$  value of a sample that can be approximated by  $\delta^{17}\text{O} \approx \frac{1}{2} \delta^{18}\text{O}$ . As a result, there was no need to measure the isotopic abundances of all three isotopes because the  $\delta^{17}\text{O}$  and  $\delta^{18}\text{O}$  values of Terrestrial materials plot on a straight line with a slope that is close to 0.5 (Fig. 3.6), and is called the Terrestrial Fractionation Line (TFL).

The close fit to the Terrestrial Fractionation Line is observed for most Earth-sourced materials. Extraterrestrial samples (Chapter 13) and terrestrial samples that have undergone photochemical reactions (Farquhar and Wing, 2003; Thiemens, 2006) often lie off of the TFL. The vertical displacement in per mil units from the TFL is the  $\Delta^{17}\text{O}$  value<sup>8</sup>, discussed below (see also Chapter 13).

When recast in a linear format (see Text box 3.1), the relationship between the  $\delta^{18}\text{O}$  and  $\delta^{17}\text{O}$  (or  $\delta^{34}\text{S}$  and  $\delta^{33}\text{S}$ ) of a set of data can be fit with a straight line of the form

$$\delta^{17}\text{O} = \lambda \delta^{18}\text{O} + \gamma \quad 3.29.$$

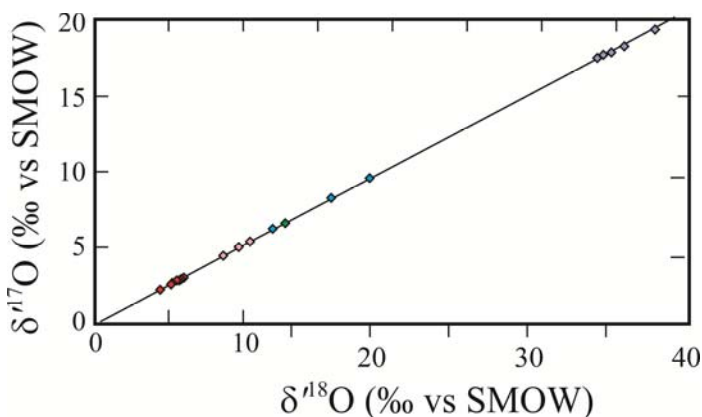


**Fig. 3.6.** Plot of the  $\delta^{17}\text{O}$  vs.  $\delta^{18}\text{O}$  values of assorted minerals from rocks of low and high temperatures. The data fall on a straight line, termed the Terrestrial Fractionation Line (TFL) with a slope =  $\lambda \approx 0.525$ . Data from Pack and Herwartz (2014).

The  $\lambda$  term is the slope of the chosen or best-fit line and the  $\gamma$  is the y intercept. (Note that the  $\gamma$  term will be equal to 0 if the best fit crosses the origin at  $\delta^{18}\text{O} = \delta^{17}\text{O} = 0$ ). Fig. 3.6 shows the results of a number of rock samples. A  $\lambda$  slope of 0.524 to 0.526 is obtained for most Earth materials (Miller, 2002; Rumble et al., 2007) with a y intercept ( $\gamma$ ) assumed to be 0. In fact,

careful analyses of terrestrial materials shows that the best fit actually has a y intercept that is slightly different from 0 (Pack and Herwartz, 2014; Sharp et al., 2016).

<sup>8</sup> In spoken English, one refers to this  $\Delta^{17}\text{O}$  as ‘Big delta’ or ‘Cap delta’, where the ‘big’ and ‘cap’ indicate a capital  $\delta$ , which is a  $\Delta$ .

The choice of  $\lambda$  is somewhat arbitrary, determined by a best fit to the data set. For rocks, the best fit results in a slope of approximately 0.525 and for meteoric water samples, the best fit results in a  $\lambda$  value of 0.528 (Luz and Barkan, 2010). The reason that there is no single 'correct value' for  $\lambda$  is that there are a number of processes that affect the triple oxygen isotope fractionation (Matsuhisa et al., 1978), and hence the relationship between  $\delta^{17}\text{O}$  and  $\delta^{18}\text{O}$ . There is no one 'correct answer' because there is no single process that determines the slope.

**Text box 3.1: Linearization of isotope data.**

Isotope data for multiple isotope systems are commonly linearized, where the  $\delta$  value is redefined in a logarithmic form and is symbolized by  $\delta'$  (pronounced 'delta prime') in place of  $\delta$ . The linearization changes the  $\delta$  values only slightly and because the delta prime values follow the relationship given by equation 3.28, linearized data will plot in a linear array in  $\delta'^{17}\text{O}$  -  $\delta'^{18}\text{O}$  space. Hulston and Thode (1965) first proposed this linearization given by

$$\delta' = 1000 \times \ln(R_{sa}/R_{std}) \quad 3B1.1$$

which, in  $\delta$  notation becomes (Miller, 2002)

$$\delta' = 1000 \times \ln(\delta/1000 + 1) \quad 3B1.2.$$

Whereas  $1000 \ln \alpha_{A-B} \approx \delta_A - \delta_B$  (equation 2.17), in a linearized format

$$1000 \ln \alpha_{A-B} = \delta'_A - \delta'_B \quad 3B1.3.$$

Under equilibrium conditions, the  $\lambda$  is replaced by  $\theta$  to indicate that the fractionation between any two phases follows well established thermodynamic rules. In some cases the  $\theta$  is also used for *reproducible* kinetic isotope fractionations (Barkan and Luz, 2007). For an equilibrium fractionation between two phases A and B with the three isotopes 1, 2, and 3,  $\theta_{A-B}$  is given by

$$\theta_{A-B} = \frac{\ln \alpha_{3/1}}{\ln \alpha_{2/1}} \quad 3.30,$$

where  $\alpha_3$  is the fractionation between the isotopes 3 and 1 (Young et al., 2002). For the triple oxygen isotope system, the equilibrium value of  $\theta$  for fractionation between quartz and water is

$$\theta_{(\text{SiO}_2-\text{H}_2\text{O})} = \frac{\ln \alpha_{(17\text{o})}}{\ln \alpha_{(18\text{o})}} = \frac{(\delta^{17}\text{O}_{\text{qz}} - \delta^{17}\text{O}_{\text{H}_2\text{O}})}{(\delta^{18}\text{O}_{\text{qz}} - \delta^{18}\text{O}_{\text{H}_2\text{O}})} \quad 3.31.$$

Graphically, the  $\theta$  value is simply the slope of the line given by the fractionation between the two phases quartz and water (Fig. 3.7).

The equations governing  $\theta$  are discussed in detail by Young *et al.* (2002). At infinite temperatures, the  $\theta$  value for the triple oxygen isotope system is given by

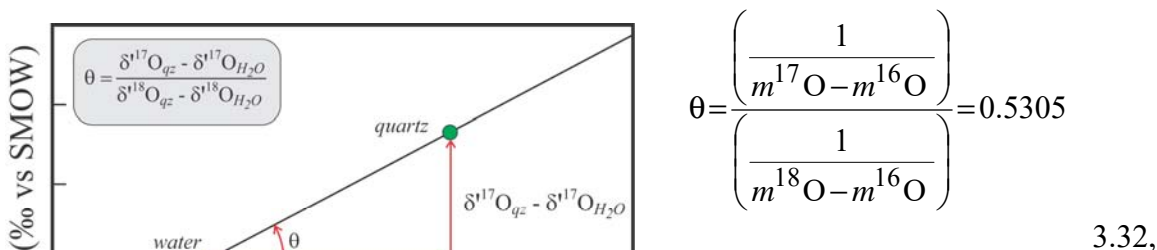


**Fig. 3.7.** Graphical representation of  $\theta$ . For two phases in isotopic equilibrium, the triple isotope fraction is given by equation 3.31. Graphically, it is equal to the slope defined by the isotopic compositions of the two phases.

where  $m^{16}\text{O}$  is the mass of  $^{16}\text{O}$ , etc. (For the three isotopes  $^{32}\text{S}$ ,  $^{33}\text{S}$ ,  $^{34}\text{S}$ , the  $\theta$  value (at infinite temperatures) is 0.5159). With decreasing temperatures, the value of  $\theta$  decreases, so that at  $0^\circ\text{C}$ , the  $\theta$  oxygen value for quartz-water fractionation is 0.524 (Cao and Liu,

2011; Sharp *et al.*, 2016). In kinetic fractionation processes, the  $\theta$  value can be as low as 0.5.

Because  $\theta$  varies with temperature and also according to the type of fractionation that has occurred (kinetic *vs.* equilibrium), the combined  $\delta^{17}\text{O}$  and  $\delta^{18}\text{O}$  values of a particular sample may plot slightly off the 'best fit' line for an assumed  $\lambda$  value. These deviations are referred to as  $\Delta^{17}\text{O}$  values (or  $\Delta^{17}\text{O}$  values in a linearized format) given by the following equation (Fig. 3.8)

$$\Delta^{17}\text{O} = \delta^{17}\text{O} - \lambda \times \delta^{18}\text{O} - \gamma \quad 3.33,$$

and more commonly

$$\Delta^{17}\text{O} = \delta^{17}\text{O} - \lambda \times \delta^{18}\text{O} \quad 3.34$$

when  $\gamma = 0$ . Although the  $\Delta^{17}\text{O}$  value will change for different assumed values of  $\lambda$ , the interpretations based on the  $\Delta^{17}\text{O}$  values will not (see Sharp *et al.*, 2016, Appendix A). The temperature dependent variations of  $\theta$  have been used as a 'single mineral thermometer' (Sharp *et al.*, 2016).

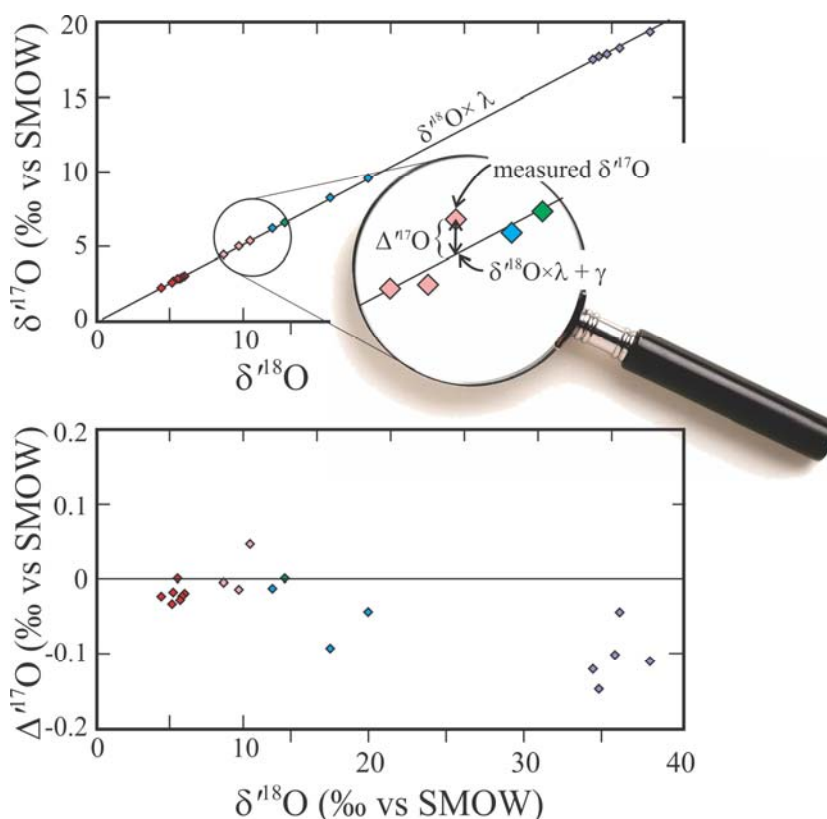


**Fig. 3.8.** Top: Illustration of small deviations from a best fit line. The vertical displacement is the  $\Delta^{17}\text{O}$  value. Bottom: When recast with  $\Delta^{17}\text{O}$  on the y-axis, subtle variations can be observed.

### 3.8 Distribution of isotopologues: Clumped Isotopes

For the simple molecule  $\text{H}_2$ , there are three possible combinations of D and H: H-H, H-D and D-D. If the two isotopes were randomly distributed in a sample of SMOW, then the abundance of each isotopologue would be the following:

$$\begin{array}{lll} \text{H}_2 = [\text{H}]^2; & \text{HD} = 2 \times [\text{H}] [\text{D}]; & \text{D}_2 = [\text{D}]^2 \\ 0.9997 & 2.979 \times 10^{-4} & 2.219 \times 10^{-8} \end{array}$$

where  $[\text{H}]$  and  $[\text{D}]$  are the fraction of each of the two isotopes. The exchange between the three isotopologues can be written as a disproportionation reaction given by  $2 \text{HD} = \text{H}_2 + \text{D}_2$ , where the equilibrium constant is  $K = \frac{[\text{H}][\text{D}]}{[\text{HD}]^2}$ . If the disproportionation were

purely stochastic (random), then  $K = 0.25$ . In fact, the molecule  $\text{D}_2$  is slightly more stable than would be expected on the basis of the reduced masses, so that sum of the energies of  $\text{D}_2$  and  $\text{H}_2$  are slightly lower than twice the energy of the  $\text{HD}$  molecule. At low temperatures, therefore,  $\text{D}_2$  and  $\text{H}_2$  will be slightly favored over  $2 \text{HD}$ . As temperatures increase the entropy of the system overwhelms the slight energy favorability of  $\text{D}_2$ , so that the  $K$  value approaches the stochastic values given above (Eiler, 2007). The

difference from the stochastic value is given by  $\Delta_i$ . The differences can be a result of temperature or kinetic fractionations (Eiler, 2007).

Clumped isotopes studies have been made on CO<sub>2</sub> (both gas and the CO<sub>2</sub> liberated from carbonates), CH<sub>4</sub> and O<sub>2</sub>. The most highly studied system is for carbonates, where the difference in the abundance of the isotopologue <sup>13</sup>C<sup>18</sup>O<sup>16</sup>O (mass 47) from the stochastic value (given by  $\Delta_{47}$ ) can be used as a single mineral thermometer (e.g., Ghosh et al., 2006). Specially configured mass spectrometers are required to measure the low abundance of the rare isotopologue <sup>13</sup>C<sup>18</sup>O<sup>16</sup>O, and long counting times are needed to get the necessary precision to make precise temperature estimates. A more detailed discussion on applications of this method are given in Chapter 7.

## References

- Barkan, E. and Luz, B. (2007) Diffusivity fractionations of  $\text{H}_2^{16}\text{O}/\text{H}_2^{17}\text{O}$  and  $\text{H}_2^{16}\text{O}/\text{H}_2^{18}\text{O}$  in air and their implications for isotope hydrology. *Rapid Communications in Mass Spectrometry* **21**, 2999-3005.
- Bigeleisen, J. and Mayer, M.G. (1947) Calculation of equilibrium constants for isotopic exchange reactions. *Journal of Chemical Physics* **15**, 261-267.
- Bird, M.I., Longstaffe, F.J., Fyfe, W.S., Tazaki, K. and Chivas, A.R. (1994) Oxygen-isotope fractionation in gibbsite: Synthesis experiments versus natural samples. *Geochimica et Cosmochimica Acta* **58**, 5267-5277.
- Blattner, P. (1975) Oxygen isotopic composition of fissure-grown quartz, adularia, and calcite from Broadlands geothermal field, New Zealand, with an appendix on quartz-K-feldspar-calcite-muscovite oxygen isotope geothermometers. *American Journal of Science* **275**, 785-800.
- Bottinga, Y. (1968) Calculation of fractionation factors for carbon and oxygen isotopic exchange in the system calcite-carbon dioxide-water. *Journal of Physical Chemistry* **72**, 800-808.
- Bottinga, Y. (1969) Carbon isotope fractionation between graphite, diamond and carbon dioxide. *Earth and Planetary Science Letters* **5**, 301-307.
- Bottinga, Y. and Javoy, M. (1973) Comments on oxygen isotope geothermometry. *Earth and Planetary Science Letters* **20**, 250-265.
- Cao, X. and Liu, Y. (2011) Equilibrium mass-dependent fractionation relationships for triple oxygen isotopes. *Geochimica et Cosmochimica Acta* **75**, 7435-7445.
- Cavosie, A., Sharp, Z.D. and Selverstone, J. (2002) Co-existing aluminum silicates in quartz veins: A quantitative approach for determining andalusite-sillimanite equilibrium in natural samples using oxygen isotopes. *American Mineralogist* **87**, 417-423.
- Chacko, T., Cole, D.R. and Horita, J. (2001a) Equilibrium oxygen, hydrogen and carbon isotope fractionation factors applicable to geologic systems, in: Valley, J.W., Cole, D.R. (Eds.), *Stable Isotope Geochemistry*. Mineralogical Society of America, Washington, D.C., pp. 1-81.
- Chacko, T., Cole, D.R. and Horita, J. (2001b) Equilibrium oxygen, hydrogen and carbon isotope fractionation factors applicable to geological systems. *Reviews in Mineralogy and Geochemistry* **43**, 1-81.
- Chacko, T., Hu, X., Mayeda, T.M., Clayton, R.N. and Goldsmith, J.R. (1996) Oxygen isotope fractionations in muscovite, phlogopite, and rutile. *Geochimica et Cosmochimica Acta* **60**, 2595-2608.
- Chacko, T., Mayeda, T.K., Clayton, R.N. and Goldsmith, J.R. (1991) Oxygen and carbon isotope fractionations between  $\text{CO}_2$  and calcite. *Geochimica et Cosmochimica Acta* **55**, 2867-2882.
- Clayton, R.N., Goldsmith, J.R., Karel, K.J., Mayeda, T.K. and Newton, R.C. (1975) Limits on the effect of pressure on isotopic fractionation. *Geochimica et Cosmochimica Acta* **39**, 1197-1201.
- Clayton, R.N., Goldsmith, J.R. and Mayeda, T.K. (1989) Oxygen isotope fractionation in quartz, albite, anorthite and calcite. *Geochimica et Cosmochimica Acta* **53**, 725-733.

- Clayton, R.N. and Kieffer, S.W. (1991) Oxygen isotopic thermometer calibrations, in: Taylor Jr., H.P., O'Neil, J.R., Kaplan, I.R. (Eds.), *Stable Isotope Geochemistry: A Tribute to Samuel Epstein*. The Geochemical Society Special Publication, pp. 1-10.
- Craig, H. (1957) Isotopic standards for carbon and oxygen and correction factors for mass-spectrometric analysis of carbon dioxide. *Geochimica et Cosmochimica Acta* **12**, 133-149.
- Criss, R.E. (1999) *Principles of stable isotope distribution*. Oxford University Press, New York.
- Denbigh, K. (1971) *The Principles of Chemical Equilibrium*, 3 ed. Cambridge University Press, Cambridge.
- Driesner, T. and Seward, T.M. (2000) Experimental and simulation study of salt effects and pressure/density effects on oxygen and hydrogen stable isotope liquid-vapor fractionation for 4-5 molal aqueous NaCl and KCl solutions at 400 degrees C. *Geochimica et Cosmochimica Acta* **64**, 1773-1784.
- Eiler, J.M. (2007) "Clumped-isotope" geochemistry—The study of naturally-occurring, multiply-substituted isotopologues. *Earth and Planetary Science Letters* **262**, 309-327.
- Epstein, S., Buchsbaum, R., Lowenstam, H. and Urey, H.C. (1951) Carbonate-water isotopic temperature scale. *Journal of Geology* **62**, 417-426.
- Epstein, S., Buchsbaum, R., Lowenstam, H.A. and Urey, H.C. (1953) Revised carbonate-water isotopic temperature scale. *Geological Society of America Bulletin* **64**, 1315-1326.
- Farquhar, J. and Wing, B.A. (2003) Multiple sulfur isotopes and the evolution of the atmosphere. *Earth and Planetary Science Letters* **213**, 1-13.
- Ghosh, P., Adkins, J., Affek, H., Balta, B., Guo, W., Schauble, E.A., Schrag, D.P. and Eiler, J.M. (2006)  $^{13}\text{C}$ - $^{18}\text{O}$  bonds in carbonate minerals: A new kind of paleothermometer. *Geochimica et Cosmochimica Acta* **70**, 1439-1456.
- Hattori, K. and Halas, S. (1982) Calculation of oxygen isotope fractionation between uranium dioxide, uranium trioxide and water. *Geochimica et Cosmochimica Acta* **46**, 1863-1868.
- Hoering, T.C. (1961) The effect of physical changes on isotopic fractionation. *Carnegie Institution of Washington Yearbook* **60**, 201-204.
- Hoffbauer, R., Hoernes, S. and Fiorentini, E. (1994) Oxygen isotope thermometry based on a refined increment method and its application to granulite-grade rocks from Sri Lanka. *Precambrian Research* **66**, 199-220.
- Horita, J., Cole, D.R., Polyakov, V.B. and Driesner, T. (2002) Experimental and theoretical study of pressure effects on hydrogen isotope fractionation in the system brucite-water at elevated temperatures. *Geochimica et Cosmochimica Acta* **66**, 3769-3788.
- Horita, J., Cole, D.R. and Wesolowski, D.J. (1993a) The activity-composition relationship of oxygen and hydrogen isotopes in aqueous salt solutions: II. Vapor-liquid water equilibration of mixed salt solutions from 50 to 100°C and geochemical implications. *Geochimica et Cosmochimica Acta* **57**, 4703-4711.
- Horita, J., Cole, D.R. and Wesolowski, D.J. (1995) The activity-composition relationship of oxygen and hydrogen isotopes in aqueous salt solutions: III. Vapor-liquid water

- equilibration of NaCl solutions to 350°C. *Geochimica et Cosmochimica Acta* **59**, 1139-1151.
- Horita, J., Wesolowski, D.J. and Cole, D.R. (1993b) The activity-composition relationship of oxygen and hydrogen isotopes in aqueous salt solutions: I. Vapor-liquid water equilibration of single salt solutions from 50 to 100°C. *Geochimica et Cosmochimica Acta* **57**, 2797-2817.
- Hu, G. and Clayton, R.N. (2003) Oxygen isotope salt effects at high pressure and high temperature and the calibration of oxygen isotope geothermometers. *Geochimica et Cosmochimica Acta* **67**, 3227-3246.
- Hulston, J.R. and Thode, H.G. (1965) Variations in the S<sup>33</sup>, S<sup>34</sup>, and S<sup>36</sup> contents of meteorites and their relation to chemical and nuclear effects. *Journal of Geophysical Research* **70**, 3475-3484.
- Kieffer, S.W. (1982) Thermodynamics and lattice vibrations in minerals: 5. Applications to phase equilibria, isotopic fractionation, and high-pressure thermodynamic properties. *Reviews of Geophysics and Space Physics* **20**, 827-849.
- Kita, I., Taguchi, S. and Matsubaya, O. (1985) Oxygen isotope fractionation between amorphous silica and water at 34-93°C. *Nature* **314**, 83-84.
- Kohn, M.J. and Valley, J.W. (1998) Oxygen isotope geochemistry of the amphiboles; isotope effects of cation substitutions in minerals. *Geochimica et Cosmochimica Acta* **62**, 1947-1958.
- Larson, T. and Sharp, Z.D. (2003) Stable isotope constraints on the Al<sub>2</sub>SiO<sub>5</sub> 'triple-point' rocks from the Proterozoic Priest pluton contact aureole, New Mexico. *Journal of Metamorphic Geology* **21**, 785-798.
- Leclerc, A.J. and Labeyrie, L. (1987) Temperature dependence of oxygen isotopic fractionation between diatom silica and water. *Earth and Planetary Science Letters* **84**, 69-74.
- Longinelli, A. and Nuti, S. (1973) Revised phosphate-water isotopic temperature scale. *Earth and Planetary Science Letters* **19**, 373-376.
- Luz, B. and Barkan, E. (2010) Variations of <sup>17</sup>O/<sup>16</sup>O and <sup>18</sup>O/<sup>16</sup>O in meteoric waters. *Geochimica et Cosmochimica Acta* **74**, 6276-6286.
- Matsuhisa, Y., Goldsmith, J.R. and Clayton, R.N. (1978) Mechanisms of hydrothermal crystallization of quartz at 250°C and 15 kbar. *Geochimica et Cosmochimica Acta* **42**, 173-182.
- Matthews, A., Goldsmith, J.R. and Clayton, R.N. (1983) On the mechanisms and kinetics of oxygen isotope exchange in quartz and feldspars at elevated temperatures and pressures. *Geological Society of America Bulletin* **94**, 396-412.
- McCrea, J.M. (1950) On the isotopic chemistry of carbonates and a paleotemperature scale. *Journal of Chemical Physics* **18**, 849-857.
- Miller, M.F. (2002) Isotopic fractionation and the quantification of <sup>17</sup>O anomalies in the oxygen three-isotope system: an appraisal and geochemical significance. *Geochimica et Cosmochimica Acta* **66**, 1881-1889.
- Morikiyo, T. (1986) Hydrogen and carbon isotope studies on the graphite-bearing metapelites in the northern Kiso District of central Japan. *Contributions to Mineralogy and Petrology* **94**, 165-177.
- Northrop, D.A. and Clayton, R.N. (1966) Oxygen-isotope fractionations in systems containing dolomite. *Journal of Geology* **74**, 174-196.

- O'Neil, J.R. (1986) Theoretical and experimental aspects of isotopic fractionation., in: Valley, J.W., Taylor Jr., H.P., O'Neil, J.R. (Eds.), *Stable Isotopes in High Temperature Geological Processes*, 1 ed. Mineralogical Society of America, Chelsea, pp. 1-40.
- O'Neil, J.R., Clayton, R.N. and Mayeda, T.K. (1969) Oxygen isotope fractionation in divalent metal carbonates. *Journal of Chemical Physics* **51**, 5547-5558.
- O'Neil, J.R. and Epstein, S. (1966) Oxygen isotope fractionation in the system dolomite-calcite-carbon dioxide. *Science* **152**, 198-200.
- O'Neil, J.R. and Taylor Jr., H.P. (1967) The oxygen isotope and cation exchange chemistry of feldspars. *American Mineralogist* **52**, 1414-1437.
- O'Neil, J.R. and Truesdell, A.H. (1991) Oxygen isotope fractionation studies of solute-water interactions, in: Taylor Jr., H.P., O'Neil, J.R., Kaplan, I.R. (Eds.), *Stable isotope geochemistry: A tribute to Samuel Epstein*. The Geochemical Society, pp. 17-25.
- Pack, A. and Herwartz, D. (2014) The triple oxygen isotope composition of the Earth mantle and  $\Delta^{17}\text{O}$  variations in terrestrial rocks. *Earth and Planetary Science Letters* **390**, 138-145.
- Perkins, G., Sharp, Z.D. and Selverstone, J. (2004) Oxygen isotopic compositions of ultramafic xenoliths from the Rio Puerco volcanic necks, NM, and implications for the source of metasomatic fluids in the lithospheric mantle. *Geological Society of America, Abstracts with Programs* **36**, 57-54.
- Polyakov, V.B. and Kharlashina, N.N. (1994) Effect of pressure on equilibrium isotopic fractionation. *Geochimica et Cosmochimica Acta* **58**, 4739-4750.
- Polyakov, V.B. and Mineev, S.D. (2000) The use of Mössbauer spectroscopy in stable isotope geochemistry. *Geochimica et Cosmochimica Acta* **64**, 849-865.
- Richet, P., Bottinga, Y. and Javoy, M. (1977) A review of hydrogen, carbon, nitrogen, oxygen, sulphur, and chlorine stable isotope fractionation among gaseous molecules. *Annual Review of Earth and Planetary Science* **5**, 65-110.
- Richter, R. and Hoernes, S. (1988) The application of the increment method in comparison with experimentally derived and calculated O-isotope fractionations. *Chemie der Erde* **48**, 1-18.
- Rubinson, M. and Clayton, R.N. (1969) Carbon-13 fractionation between aragonite and calcite. *Geochimica et Cosmochimica Acta* **33**, 997-1002.
- Rumble, D., Miller, M.F., Franchi, I.A. and Greenwood, R.C. (2007) Oxygen three-isotope fractionation lines in terrestrial silicate minerals: An inter-laboratory comparison of hydrothermal quartz and eclogitic garnet. *Geochimica et Cosmochimica Acta* **71**, 3592-3600.
- Savin, S.M. and Epstein, S. (1970) The oxygen and hydrogen isotope geochemistry of clay minerals. *Geochimica et Cosmochimica Acta* **34**, 25-42.
- Savin, S.M. and Lee, M. (1988) Isotopic studies of phyllosilicates, in: Bailey, S.W. (Ed.), *Hydrous phyllosilicates*. Mineralogical Society of America, Chelsea, pp. 189-223.
- Schauble, E.A. (2004) Applying stable isotope fractionation theory to new systems, in: Johnson, C.M., Beard, B.L., Albarède, F. (Eds.), *Geochemistry of Non-Traditional Stable Isotopes*. Mineralogical Society of America, Washington, D.C., pp. 65-111.
- Schütze, H. (1980) Der Isotopenindex -- eine Inkrementenmethode zur näherungsweise Berechnung von Isotopenaustauschgleichgewichten zwischen kristallinen Substanzen. *Chemie der Erde* **39**, 321-334.

- Sharp, Z.D. (1995) Oxygen isotope geochemistry of the Al<sub>2</sub>SiO<sub>5</sub> polymorphs. *American Journal of Science* **295**, 1058-1076.
- Sharp, Z.D., Essene, E.J. and Smyth, J.R. (1992) Ultra-high temperatures from oxygen isotope thermometry of a coesite-sanidine grosspydite. *Contributions to Mineralogy and Petrology* **112**, 358-370.
- Sharp, Z.D., Gibbons, J.A., Maltsev, O., Atudorei, V., Pack, A., Sengupta, S., Shock, E.L. and Knauth, L.P. (2016) A calibration of the triple oxygen isotope fractionation in the SiO<sub>2</sub> - H<sub>2</sub>O system and applications to natural samples. *Geochimica et Cosmochimica Acta* **186**, 105-119.
- Smyth, J.R. (1989) Electrostatic characterization of oxygen sites in minerals. *Geochimica et Cosmochimica Acta* **53**, 1101-1110.
- Stolper, E. and Epstein, S. (1991) An experimental study of oxygen isotope partitioning between silica glass and CO<sub>2</sub> vapor, in: Taylor Jr., H.P., O'Neil, J.R., Kaplan, I.R. (Eds.), *Stable Isotope Geochemistry: A Tribute to Samuel Epstein*. The Geochemical Society, San Antonio, pp. 35-51.
- Suzuoki, T. and Epstein, S. (1976) Hydrogen isotope fractionation between OH-bearing minerals and water. *Geochimica et Cosmochimica Acta*. **40**, 1229-1240.
- Taylor, B.E. and O'Neil, J.R. (1977) Stable isotope studies of metasomatic skarns and associated metamorphic and igneous rocks, Osgood Mountains, Nevada. *Contributions to Mineralogy and Petrology* **63**, 1-49.
- Taylor, H.P., Jr. and Epstein, S. (1962) Relationship between O<sup>18</sup>/O<sup>16</sup> ratios in coexisting minerals of igneous and metamorphic rocks Part 1. Principles and experimental results. *Geological Society of America Bulletin* **73**, 461-480.
- Thiemens, M. (2006) History and applications of mass-independent isotope effects. *Annual Reviews of Earth and Planetary Sciences* **34**, 217-262.
- Young, E.D., Galy, A. and Nagahara, H. (2002) Kinetic and equilibrium mass-dependent isotope fractionation laws in nature and their geochemical and cosmochemical significance. *Geochimica et Cosmochimica Acta* **66**, 1095-1104.
- Zheng, Y.-F., Metz, P. and Satir, M. (1994a) Oxygen isotope fractionation between calcite and tremolite: an experimental study. *Contributions to Mineralogy and Petrology* **118**, 249-255.
- Zheng, Y.F. (1993) Calculation of oxygen isotope fractionation in anhydrous silicate minerals. *Geochimica et Cosmochimica Acta* **57**, 1079-1091.
- Zheng, Y.F., Metz, P., Satir, M. and Sharp, Z.D. (1994b) An experimental calibration of oxygen isotope fractionation between calcite and forsterite in the presence of a CO<sub>2</sub>-H<sub>2</sub>O fluid. *Chemical Geology* **116**, 17-27.